ACS Macro Letters

Letter

pubs.acs.org/macroletters

Room Temperature Synthesis of a Covalent Monolayer Sheet at Air/Water Interface Using a Shape-Persistent Photoreactive Amphiphilic Monomer

Yougen Chen,[§] Ming Li,[§] Payam Payamyar, Zhikun Zheng, Junji Sakamoto,[†] and A. Dieter Schlüter*

Laboratory of Polymer Chemistry, Department of Materials, Swiss Federal Institute of Technology, ETH Zürich, HCI J 541, CH-8093 Zürich, Switzerland

Supporting Information

ABSTRACT: The shape-persistent monomer **3** with its three 1,8-diazaanthracene (DAA) units is spread and compressed at the air/water interface and the layer then converted into a 1.5 nm thick covalent monolayer sheet by photoirradiation under ambient conditions. The sheet obtained under these extremely mild conditions is mechanically stable to carry its own weight when spanned over TEM grids. While its molecular structure cannot be given yet with certainty, it is likely to be the result of [4 + 4]-cycloaddition dimerizations between the DAA units of neighboring monomers. Evidence is based on the wavelength of the monomer fluorescence emission, the kinetics of this emission's intensity decay with irradiation time, and the mechanical sheet stability that suggests a surpassing of percolation threshold. Finally, the thermal stability of the sheet is investigated.

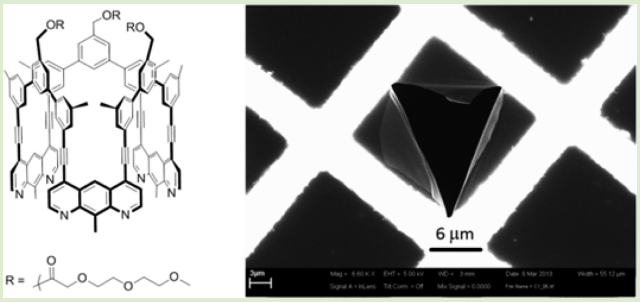

Monolayer or sheet-like covalent polymers in which the monomer units are periodically connected in two dimensions are fascinating objects for physicists and chemists. Due to their particular dimensionality, they are believed to show unique properties different from known 3D materials, thus, enabling potential applications in fields such as single-molecule electronics,[1−3] semiconductors,[4,5] ultrasensitive sensors,[5] optoelectronic devices,[6−8] nanosieves,[9] nanomembranes,[10−14] cell engineering,[15,16] medicines,[16] and molecular machines.[17] According to a recently advertised definition, such polymers have topologically planar repeat units and are referred to as two-dimensional polymers (2DP).[18] For a somewhat differing definition recently put forward by the Dichtel group, see ref 19. Research in the direction of 2DP and less strictly defined, covalent monolayer sheets have gained considerable momentum since the discovery of graphene, a natural 2DP, with its fascinating properties. Pioneering work in creating ultrathin covalent sheets dates back to the mid-1930s when multifunctional monomers were confined into two dimensions at the air/water interface before being irregularly cross-linked into sheets.[20] Thereafter, numerous efforts were devoted to create covalent monolayer sheets of various sorts at interfaces (air/liquid, liquid/liquid) on solid substrates and by wet-chemical approaches in solution.[21−24] While these attempts afforded invaluable scientific insights and even new materials, they did not lead to a 2DP according to the above definition with sizes that would exceed a few tenth of nanometers. Based on monomer **1** (Figure 1), our laboratory has recently reported the first proven case of a 2DP with sizes in the micrometer range.[25] Shortly after, this was followed by a second case from the King laboratory.[26] Because these two 2DP cases rest upon the single crystal approach, structure elucidation was comparably easy. We also reported a variety of covalent and metal−organic monolayer sheets at the air/water interface.[27−30] Determining the internal structure of those sheets is a more challenging matter because, in contrast to the single crystal approach, the structure of the monomer assembly at the interface, and thus the starting situation, is not normally known. The covalent monolayer sheet reported here was obtained from the amphiphilic monomer **2**.[31] This monomer was spread and compressed at the air/water interface and the resulting array was then irradiated directly at the interface. There is evidence from fluorescence spectroscopy that the monomers assume a relative orientation such that the anthracenes of neighboring monomers are face-to-face (*ftf*) stacked. Such stacking would allow for the well-known photochemically initiated [4 + 4]-cycloaddition to take place at the 9,10-positions within each pair of anthracenes so as to convert the monomer layer directly into the covalent sheet counterpart. While the structure elucidation is still being completed, the sheets, which shall be referred to as **S2**, were obtained in the cm^2-range and with a mechanical coherence that allowed spanning those over 20 × 20 μm^2-sized holes. Thus, within each hole approximately 10^7 molecules could be connected to one another strictly within two dimensions such that they support their own weight, and the process that made this happen was run under mild

Received: November 25, 2013
Accepted: January 13, 2014
Published: January 15, 2014

   dx.doi.org/10.1021/mz400597k | *ACS Macro Lett.* 2014, 3, 153−158

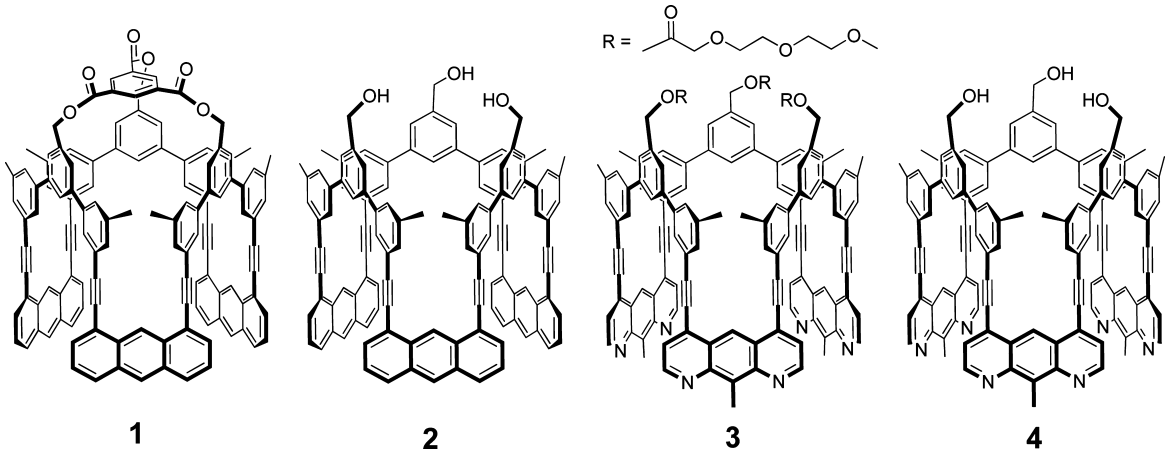

Figure 1. Chemical structures of anthracene- and 1,8-diazaanthracene-based monomers for two-dimensional polymer synthesis.[25,31,33]

conditions (typically room temperature). This mildness is an important feature which sets **S2** and other sheets apart from many inorganic congeners such as graphene, MoS_2, BN, and WSe_2, whose syntheses often require harsh, for example, pyrolytic, conditions. Consequently, because monomer **2** has three hydroxyl groups, one side of sheet **S2** over its entire expanse presents densely spaced hydroxyl groups, which invite themselves for chemical modification. The other side of **S2** is composed of hydrophobic anthracene dimers rendering the sheet a 2D Janus-type object.[32] Recently we have reported the synthesis of monomer **4**, which differs from **2** mainly by the presence of 1,8-diazaanthracene (DAA) instead of parent anthracenes. This synthesis was carried out not only to broaden the structural basis for the important approach to sheets of kind **S2** but also with the idea in mind to provide a covalent sheet, **S4**, whose both sides can in principle be functionalized, perhaps even independently from one another.

We here give a preliminary account on the spreadability of monomer **4** which made us divert to its closely related, OEG-modified congener **3**, the interfacial behavior of **3** in terms of surface pressure/area isotherms and Brewster angle microscopy (BAM) imaging, the UV-initiated polymerization of the monolayer and the spanning behavior of the resulting sheet **S3**. Finally, first stability tests under increased temperatures will be reported.

Initial spreading experiments were performed with compound **4**. Quickly it was discovered that its solubility in low boiling solvents such as chloroform or hexane was insufficient to obtain homogeneous monomer layers at the air/water interface. It was therefore decided to convert the three hydroxyl groups of **4** into short OEG chains. This should maintain the required amphiphilicity but also prevent hydrogen bond formation between DAA units and free hydroxyl groups which was seen as the cause for the poor solubility in solvents of low polarity. Monomer **3** was readily obtained by esterifying compound **4** with freshly prepared 2-(2-(2-methoxyethoxy)ethoxy)acetyl chloride in a 34% yield after preparative TLC purification (see SI). For spreading, a chloroform solution of monomer **3** (1 mg/mL) was gently dropped onto the water surface. The surface pressure/mean molecular area (SP/MMA) isotherms were recorded with compression and found to be fully reproducible in independent runs (Figure 2a). From the isotherm, the MMA of monomer **3** was estimated to be about 220 Å^2. This value is close to the one reported for monomer **2** which, given the very closely related structures, is reasonable.

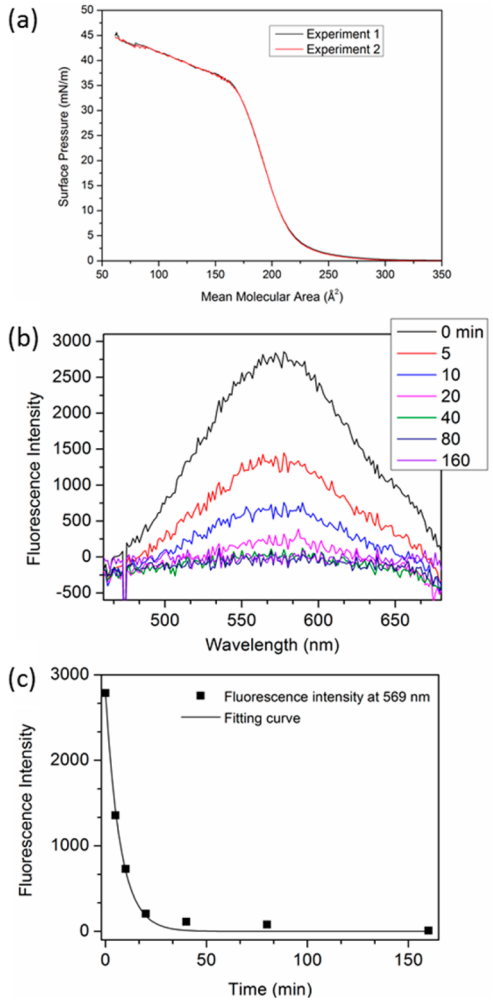

Figure 2. Monomer **3** at the air/water interface: (a) Surface pressure (SP) versus mean molecular area (MMA) isotherm. (b) In situ fluorescence emission spectra (excitation wavelength at λ = 365 nm). (c) Intensity of maximum fluorescence emission at λ = 569 nm in dependence of irradiation time. Fluorescence intensity in a.u.

We therefore tentatively assume that also the packing model discussed for monomer **2** holds true here,[31] though further proof will be required in the future. In this (idealized) model, the monomers assume a trigonal conformation with all DAAs of a given monomer *ftf* stacking with neighboring DAAs.

dx.doi.org/10.1021/mz400597k | *ACS Macro Lett.* 2014, 3, 153−158

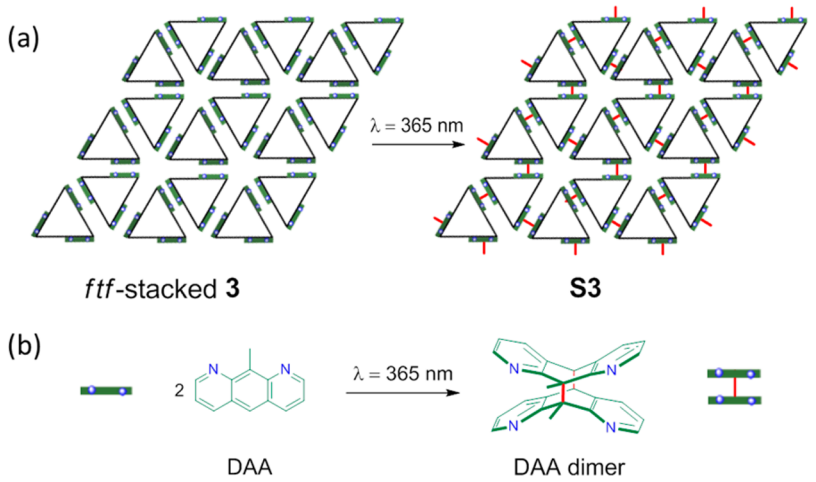

Figure 3. (a) An idealized representation of the photochemical polymerization of monomer **3** (shown in a triangular conformation) into the covalent monolayer 2D sheet **S3** by photoirradiation. (b) The connection chemistry is likely to be the depicted *syn*-dimerization of the monomers' DAA units.

Directly after spreading the monomer, well-separated domains were visible under the Brewster-angle microscope (BAM), as judged by the different gray tones in the image shown in Figure S2. Upon compression, the domains continuously coalesced to eventually form a homogenously distributed layer of monomer **3** when SP reached 12 mN/m (Figure S2). The layer finally started to collapse when SP reached the range of 30 mN/m. Based on this analysis, all further experiments were performed at SP = 15 mN/m.

The UV−vis absorption and emission spectra of monomer **3** obtained in chloroform solution and at the air/water interface are shown in Figure S3 (see also Figure 2b). The absorption bands of monomer **3** in the *p*-band region are localized in the range of λ = 360−465 nm, which is typical for DAAs solely interacting with solvent molecules.[34] In the emission spectra, the fluorescence of monomer **3** obtained in 1 μM chloroform solution displayed a maximum emission at λ = 480 nm. In contrast, the fluorescence at the air/water interface suffered a large bathochromic shift with the emission maximum now at λ = 569 nm. This substantial shift indicates that the DAA units in the monolayer of monomer **3** are either engaged in excimers or tightly *ftf* stacked pairs.[35]

Next the thickness of the layer at the interface needed to be determined. Because it is demanding to actually do so at the interface, for example, by neutron reflectivity, we transferred the layer in a vertical mode onto 285 nm SiO_2-coated silicon substrate. This transfer was rather successful as was concluded from the optical microscopy (OM) image in Figure S3 where several hundred μm large pieces of layer can be seen. These pieces have a uniform color contrast indicating homogeneity at the length scale of visible light. The cracks between the pieces were used to determine tapping mode AFM heights, h_{AFM}. The positions at which these measurements were conducted are displayed in Figures S4 and resulted in h_{AFM} = 1.5 nm. Despite the uncertainties with TM-AFM height determinations,[36] this value is in excellent agreement with the calculated height of monomer **3** (h_{calc} = 1.5 nm, Figure S4) assuming that the flexible OEG chains lie more or less flat on the substrate. Other options include helical conformations of the OEG chains or their positioning inside the monomer cavity. Thus, after transfer, the monomer forms a monolayer and it is likely that it does the same at the interface.

All polymerizations of **3** were directly carried out at air/water interface under the conditions of room temperature, SP = 15 mN/m, and excitation wavelength λ_{ex} = 365 nm (Figure 3). Assuming in a first approximation that there is no energy transfer within the monolayer resulting in enhanced emission intensity, the fluorescence intensity (I) should be proportional to the number of unreacted DAA moieties (A) within the region exposed to the UV light. We therefore monitored the fluorescence decay in dependence of irradiation time for the whole polymerization process (Figure 2b). The fluorescence emission decreased continuously, reaching negligible values after a 160 min irradiation, indicating the completion of [4 + 4]-cycloaddition dimerization across the DAA 9,10-positions between neighboring monomers. Note that the irradiation time strongly depends on the particular setup of LED, interface, and detector. The *I* values at maximum emission (569 nm) were plotted against irradiation time (Figure 2c) and could be fitted well with the exponential function in eq 1:

$$I = I_0 e^{-kt} \quad (1)$$

where I_0, *k*, and *t* are the initial *I* at 0 min (I_0 = 2771.9), rate constant (k = −0.1366), and irradiation time (min). Assuming $I \sim A$, it follows

$$I = KA \quad (2)$$

where *K* is the proportionality constant between real-time *I* and *A*. On the basis of eqs 1 and 2, *A* can be formulated as

$$A = (I_0/K)e^{-kt} \quad (3)$$

which is a typical equation for first-order reaction. This suggests that the photopolymerization of **3** at air/water interface is in fact of first-order supporting the view of DAA pairs or excimers. Based on eq 3, the polymerization can reach very high completion within 60 min. It should be noted that the polymerization was carried out under ambient. This may raise the question whether oxygen should not interfere. Photochemically initiated reactions between anthracene and DAA units and molecular oxygen are well established.[37] While at the present stage we cannot exclude the interference of oxygen altogether, we would like to point to the fact that also in the polymerization of monomer **2** there was no indication for any sizable impact of oxygen. Furthermore, when studying photochemical oxidation of anthracene in solution there is a

dx.doi.org/10.1021/mz400597k | *ACS Macro Lett.* 2014, 3, 153−158

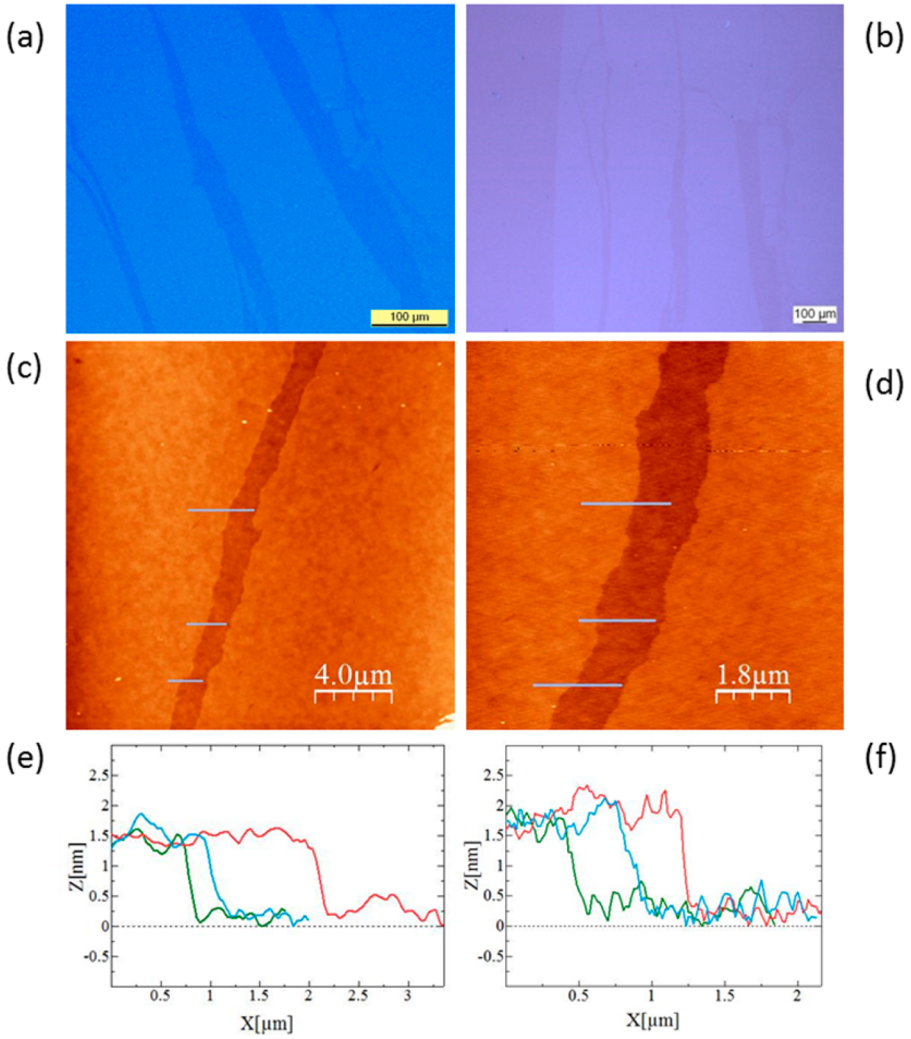

Figure 4. Sheet **S3** after transfer on 285 nm SiO_2-coated silicon: (a, b) Optical microscopy (OM) images; (c, d) Tapping mode atomic force microscopy (AFM) height images with the corresponding height profiles (e) and (f) that show some variation in the apparent thickness.

concentration beyond which dimerization is clearly taking over oxidation resulting in pure dimer and no oxidation product.[37c] In this sense, though not directly comparable, we consider our monolayers as maximally concentrated DAA units.

The sheets **S3** were vertically transferred onto 285 nm SiO_2-coated silicon substrates, and investigated by OM and AFM. OM revealed again a homogeneous color contrast and the huge sheet size in the range of hundreds of μm (Figure 4a,b). Figure 4 shows cracks that were used for AFM height determination and also provides height profiles resulting in h_{AFM} (**S3**) = 1.5−1.7 nm. These values are very similar to the aforediscussed monomer monolayer, indicating that the obtained sheet **S3** is in fact a monolayer whose thickness remained virtually unchanged by the polymerization. This is in line with the mechanistic assumption of a [4 + 4]-cycloaddition. To test its mechanical stability, **S3** was also transferred onto regular transmission electron microscopy (TEM) grids with 20 × 20 μm^2 holes and observed under scanning electron microscopy (SEM). Figure S7 provides three different magnifications. Most of the holes are completely spanned. Occasionally there are ruptures that we assign either to drying effects or stresses during transfer and to beam sensitivity. A control experiment (Figure S7d) ascertained that the monolayer of monomer **3** without being irradiated cannot span the same holes.

Prompted by the well-known fact that a retro-[4 + 4] cycloaddition of anthracene dimers into the two anthracenes can be thermally induced, the thermal stability of the sheet **S3** while spanned over a TEM grid was investigated. Figure S5 shows the SEM images of the same **S3** after exposure for different temperatures and duration in the ambient (r.t., 2 h; 120 °C, 12 h; 200 °C, 90 h). Obviously the sheet is stable even under the most forcing conditions. The only change that is observed is wrinkle formation at 200 °C, which most likely is a reflection of the different thermal expansion coefficients of sheet and Cu grid. Interestingly, in solution DAA dimers are known to undergo retro-reaction already at approximately 120 °C.[38] This suggests that the retro-reaction in a sheet faces higher activation barriers presumably resulting from the fact that each retro-step has to happen against the network, which rather prefers to keep everything in position in order to avoid local stresses.

The DAA-based monomer **3** when compressed at the air/water interface to SP = 15 mN/m upon photoirradiation converts into a covalent monolayer sheet which most likely is held together by the formation of DAA dimers between adjacent monomers. This is in line with a large bathochromic shift of the fluorescence signal when at the interface, the first-order kinetics of the fluorescence intensity decay and the fact that the sheet is

dx.doi.org/10.1021/mz400597k | *ACS Macro Lett.* 2014, 3, 153−158

mechanically coherent and stable enough to be spanned over 20 × 20 μm^2 holes. Ideally, the sheet formed has an Archimedean 6^3 type lattice for which the percolation threshold is 65%. Mechanical strength is thus expected to only start building up for polymerization conversions beyond this threshold. We thus conclude that the polymerization to sheet **S3** proceeded to a high conversion, in line with the complete disappearance of fluorescence intensity. Sheet **S3** has a surprisingly high thermal stability which shows that solution data and reversibility of chemical reactions cannot automatically be applied to sheets where internal stresses have a non-negligible impact. Sheet **S3** has two different sides. One is characterized by a dense array of short OEG "hairs", while the other exposes the DAA nitrogen atoms. There is ample evidence for ether cleavage reactions as well as functionalization of nitrogen-based hetaromatics of the pyridine[39] type so that the present work lays the foundation for a systematic exploration of postpolymerization modification on both sides of the same sheet. The mechanical stability of sheet **S3** is reflected by the ability to span huge holes. Presently the mechanical characteristics of **S3** are being determined by AFM indentation experiments.

■ ASSOCIATED CONTENT

Ⓢ Supporting Information

Materials and instruments used, synthesis of monomer **3**, BAM images of spread monomer **3**, OM images of transferred monomer monolayer, UV spectrum of monomer **3** in solution and at interface, AFM height profiles of sheet **S3** on silicon, and OM images of the changes of sheet **S3** upon thermal treatment. This material is available free of charge via the Internet at http://pubs.acs.org.

■ AUTHOR INFORMATION

Corresponding Author

*E-mail: ads@mat.ethz.ch.

Present Address

[†]Department of Applied Chemistry, Graduate School of Engineering, Osaka University, 2−1 Yamadaoka, Suita, 565−0871 Osaka, Japan (J.S.).

Author Contributions

[§]Authors contributed equally.

Notes

The authors declare no competing financial interest.

■ ACKNOWLEDGMENTS

We thank Prof. T. Kakuchi, Hokkaido University, Sapporo, Japan, for his kind support of this research. We thank Prof. N. D. Spencer, ETHZ, for access to his AFM, Prof. P. Smith and Dr. K. Feldman, both ETHZ, for their help with their optical microscopes and further support, and Ms. K. Junker and J. Rao for their kind help in AFM, UV−vis, and fluorescence measurements. This work was supported by ETH Research Grant ETH-26 10-2, which is gratefully acknowledged.

■ REFERENCES

(1) Novoselov, K. S.; Falko, V. I.; Colombo, L.; Gellert, P. R.; Schwab, M. G.; Kim, K. *Nature* **2012**, *490*, 192−200.

(2) Pang, S.; Hernandez, Y.; Feng, X.; Müllen, K. *Adv. Mater.* **2011**, *23*, 2779−2795.

(3) Kim, M.; Hohman, J. N.; Cao, Y.; Houk, K. N.; Ma, H.; Jen, A. K.-Y.; Weiss, P. S. *Science* **2011**, *331*, 1312−1315.

(4) Bangert, U.; Pierce, W.; Kepaptsoglou, D. M.; Ramasse, Q.; Zan, R.; Gass, M. H.; Van den Berg, J. A.; Boothroyd, C. B.; Amani, J.; Hofsass, H. *Nano Lett.* **2013**, *13*, 4902−4907.

(5) Lopez-Sanchez, O.; Lembke, D.; Kayci, M.; Radenovic, A.; Kis, A. *Nat. Nanotechnol.* **2013**, *8*, 497−501.

(6) High, A. A.; Novitskaya, E. E.; Butov, L. V.; Hanson, M.; Gossard, A. C. *Science* **2008**, *321*, 229−231.

(7) Kim, K. S.; Zhao, Y.; Jang, H.; Lee, S. Y.; Kim, J. M.; Kim, K. S.; Ahn, J.-H.; Kim, P.; Choi, J.-Y.; Hong, B. H. *Nature* **2009**, *457*, 706−710.

(8) Lin, Y. M.; Jenkins, K. A.; Valdes-Garcia, A.; Small, J. P.; Farmer, D. B.; Avouris, P. *Nano Lett.* **2009**, *9*, 422−426.

(9) Choi, D.-H.; Han, Y. D.; Lee, B.-K.; Choi, S.-J.; Yoon, H. C.; Lee, D.-S.; Yoon, J.-B. *Adv. Mater.* **2012**, *24*, 4408−4413.

(10) Bunch, J. S.; Verbridge, S. S.; Alden, J. S.; van der Zande, A. M.; Parpia, J. M.; Craighead, H. G.; McEuen, P. L. *Nano Lett.* **2008**, *8*, 2458−2462.

(11) Koenig, S. P.; Boddeti, N. G.; Dunn, M. L.; Bunch, J. S. *Nat. Nanotechnol.* **2011**, *6*, 543−546.

(12) Jiang, D. E.; Cooper, V. R.; Dai, S. *Nano Lett.* **2009**, *9*, 4019−4024.

(13) Schrier, J. *J. Phys. Chem. Lett.* **2010**, *1*, 2284−2287.

(14) Nair, R. R.; Wu, H. A.; Jayaram, P. N.; Grigorieva, I. V.; Geim, A. K. *Science* **2012**, *335*, 442−444.

(15) Mohanty, N.; Fahrenholtz, M.; Nagaraja, A.; Boyle, D.; Berry, V. *Nano Lett.* **2011**, *11*, 1270−1275.

(16) Yao, J.; Sun, Y.; Yang, M.; Duan, Y. X. *J. Mater. Chem.* **2012**, *22*, 14313−14329.

(17) Clemente-Leon, M.; Credi, A.; Martinez-Diaz, M. V.; Mingotaud, C.; Stoddart, J. F. *Adv. Mater.* **2006**, *18*, 1291−1296.

(18) Sakamoto, J.; van Heijst, J.; Lukin, O.; Schlüter, A. D. *Angew. Chem., Int. Ed.* **2009**, *48*, 1030−1069.

(19) Colson, J. W.; Dichtel, W. R. *Nat. Chem.* **2013**, *5*, 453−465 The definition suggested in this reference does not restrict 2DPs to monolayers but rather also involves sheet aggregates and layered crystals. We feel that the full potential of a 2DP is realized when they are isolated as individual sheets. The miraculous nature of graphene was not appreciated before isolating it as free-standing sheets from graphite. We consider this graphene analogy more appropriate to illustrate what a 2DP is and what not than the analogy between 2DPs and 1D polymers drawn in this reference. This recent definition would consider both graphene and graphite a 2DP. While this is topologically correct, it fails to emphasize what makes 2DPs special; they are persistent two-dimensional rather than one- or three-dimensional objects. Thin sheet aggregates are undoubtedly useful materials and we therefore suggest using the term 2D material for them instead of 2DP to make the difference clear between multiple and single sheets. 2DP would thus be a particular 2D material.

(20) (a) Gee, G.; Rideal, E. K. *Proc. R. Soc. London, Ser. A* **1935**, *153*, 116−128. (b) Gee, G. *Trans. Faraday Soc.* **1936**, *32*, 187−195. (c) Gee, G.; Rideal, E. K. *J. Chem. Soc.* **1937**, 772−778.

(21) Sakamoto, J.; Schlüter, A. D. In *Synthesis of Polymers, New Structures and Methods*; Schlüter, A. D., Hawker, C. J., Sakamoto, J., Eds.; Wiley-VCH: Weinheim, Germany, 2012; Vol. *2*, p 841.

(22) (a) Asakusa, S.; Okada, H.; Kunitake, T. *J. Am. Chem. Soc.* **1991**, *113*, 1749−1755. (b) Stupp, S. I.; Son, S.; Lin, H. C.; Li, L. S. *Science* **1993**, *259*, 59−63. (c) Stupp, S. I.; Son, S.; Li, L. S.; Lin, H. C.; Keser, M. *J. Am. Chem. Soc.* **1995**, *117*, 5212−5227.

(23) (a) Perepichka, D. F.; Rosei, F. *Science* **2009**, *323*, 216−217. (b) Grill, L.; Dyer, M.; Lafferentz, L.; Persson, M.; Peters, M. V.; Hecht, S. *Nat. Nanotechnol.* **2007**, *2*, 687−691.

(24) (a) Bieri, M.; Treier, M.; Cai, J.; Ait-Mansour, K.; Ruffieux, P.; Groning, O.; Groning, P.; Kastler, M.; Rieger, R.; Feng, X.; Müllen, K.; Fasel, R. *Chem. Commun.* **2009**, *45*, 6919−6921. (b) Cai, J.; Ruffieux, P.; Jaafar, R.; Bieri, M.; Braun, T.; Blankenburg, S.; Muoth, M.; Seitsonen, A. P.; Saleh, M.; Feng, X.; Müllen, K.; Fasel, R. *Nature* **2010**, *466*, 470−473. (c) Bartels, L. *Nat. Chem.* **2010**, *2*, 87−95. (d) Kley, C. S.; Cechal, J.; Kumagai, T.; Schramm, F.; Ruben, M.; Stepanow, S.; Kern, K. *J. Am. Chem. Soc.* **2012**, *134*, 6072−6075.

(e) Bieri, M.; Blankenburg, S.; Kivala, M.; Pignedoli, C. A.; Ruffieux, P.; Müllen, K.; Fasel, R. *Chem. Commun.* **2011**, *47*, 10239−10241. (f) Abel, M.; Clair, S.; Ourdjini, O.; Mossoyan, M.; Porte, L. *J. Am. Chem. Soc.* **2011**, *133*, 1203−1205. (g) Lafferentz, L.; Eberhardt, V.; Dri, C.; Africh, C.; Comelli, G.; Esch, F.; Hecht, S.; Grill, L. *Nat. Chem.* **2012**, *4*, 215−220. Cardenas, L.; Gutzler, R.; Lipton-Duffin, J.; Fu, C.; Brusso, J. L.; Dinca, L. E.; Vondrácek, M.; Fagot-Revurat, Y.; Malterre, D.; Rosei, F.; et al. *Chem. Sci.* **2013**, *4*, 3263−3268.

(25) Kissel, P.; Erni, R.; Schweizer, W. B.; Rossell, M. D.; King, B. T.; Bauer, T.; Götzinger, S.; Schlüter, A. D.; Sakamoto, J. *Nat. Chem.* **2012**, *4*, 287−291.

(26) Bhola, R.; Payamyar, P.; Murray, D. J.; Kumar, B.; Teator, A. J.; Schmidt, M. U.; Hammer, S. M.; Saha, A.; Sakamoto, J.; Schlüter, A. D.; King, B. T. *J. Am. Chem. Soc.* **2013**, *135*, 14134−14141.

(27) Bauer, T.; Zheng, Z. K.; Renn, A.; Enning, R.; Stemmer, A.; Sakamoto, J.; Schlüter, A. D. *Angew. Chem., Int. Ed.* **2011**, *50*, 7879−7884.

(28) Schlüter, A. D.; Sakamoto, J. *Pure Appl. Chem.* **2012**, *84*, 861−867.

(29) Payamyar, P.; Sakamoto, J.; Schlüter, A. D. *Chimia* **2013**, *67*, 283−285.

(30) Zheng, Z.; Ruiz-Vargas, C. S.; Bauer, T.; Rossi, A.; Payamyar, P.; Schütz, A.; Stemmer, A.; Sakamoto, J.; Schlüter, A. D. *Macromol. Rapid Commun.* **2013**, *34*, 1670−1680.

(31) Payamyar, P.; Kaja, K.; Ruiz-Vargas, C.; Stemmer, A.; Murray, D. J.; Johnson, C.; King, B. T.; Schiffmann, F.; VandeVondele, J.; Renn, A.; Götzinger, S.; Ceroni, P.; Schütz, A.; Lee, L.-T.; Zheng, Z.; Sakamoto, J.; Schlüter, A. D. *Adv. Mater.* **2014**, DOI: 10.1002/adma.201304705.

(32) Walter, A.; Müller, A. H. E. *Chem. Rev.* **2013**, *113*, 5194−5261.

(33) Li, M.; Klärner, F.-G.; Sakamoto, J.; Schlüter, A. D. *Chem.—Eur. J.* **2013**, *19*, 13348−13354.

(34) Berni, E.; Huc, I.; Kauffmann, B.; Léger, J.-M.; Zhan, C.; Huc, I. *J. Org. Chem.* **2008**, *73*, 2687−2694.

(35) (a) Hayashi, T.; Mataga, N.; Sakata, Y.; Misumi, S.; Morita, M.; Tanaka, J. *J. Am. Chem. Soc.* **1976**, *98*, 5910−5913. (b) Branchi, B.; Ceroni, P.; Balzani, V.; Cartagena, M. C.; Klärner, F.-G.; Schrader, T.; Vögtle, F. *New J. Chem.* **2009**, *33*, 397−407.

(36) For example, see: Zhuang, W.; Ecker, C.; Metselaar, G. A.; Rowan, A. E.; Nolte, R. J. M.; Samori, P.; Rabe, J. P. *Macromolecules* **2005**, *38*, 473−480.

(37) (a) For example, see: Fudickar, T. L. *Langmuir* **2010**, *26*, 4421−4428. (b) Bouas-Laurent, H.; Castellan, A.; Desvergne, J. P.; Lapouyade, R. *Chem. Soc. Rev.* **2000**, *29*, 43−55. (c) Bouas-Laurent, H.; Castellan, A.; Desvergne, J. P.; Lapouyade, R. *Chem. Soc. Rev.* **2001**, *30*, 248−263. (d) Kitahara, K.; Nishi, H. *J. Heterocycl. Chem.* **1988**, *25*, 1063−1065.

(38) For a retro-cycloaddition of a related DAA dimer, see: Li, M.; Schlüter, A. D.; Sakamoto, J. *J. Am. Chem. Soc.* **2012**, *134*, 11721−11725.

(39) (a) Renotte, R.; Sarlet, G.; Thunus, L.; Lejeune, R. *Luminescence* **2000**, *15*, 311−320. (b) Ezquerra, J.; Alvarez-Builla, J. *J. Heterocycl. Chem.* **1986**, *23*, 1151−1157. (c) Parenty, A. D. C.; Smith, L. V.; Cronin, L. *Tetrahedron* **2005**, *61*, 8410−8418. (d) Barbaras, D.; Kaiser, M.; Brun, R.; Gademann, K. *Bioorg. Med. Chem. Lett.* **2008**, *18*, 4413−4415. (e) Mehranpour, A. M.; Hashemnia, S.; Azamifar, F. *Tetrahedron Lett.* **2013**, *54*, 321−323.